PHYSICAL REVIEW B VOLUME 24, NUMBER 1 1 JULY 1981

Hypernetted-chain indications of phase transitions in the ^{4}He and charged-Bose systems

A. D. Jackson, B. K. Jennings, and R. A. Smith
Department of Physics, SUNY at Stony Brook, New York, 11794

A. Lande
Institute for Theoretical Physics, University of Groningen, Groningen, The Netherlands

(Received 25 September 1979; revised manuscript received 16 June 1980)

Optimal hypernetted-chain (HNC) methods provide a useful approach to the study of the liquid state of many-body systems. They give reasonable numerical results and yet many analytical manipulations may be made with them. Previously, the behavior of the energy functional in an infinitesimal region of the optimal liquid correlation function was studied. This eigenvalue analysis reliably characterized the droplet formation of liquid ^{4}He at the spinodal point and indicated the possibility of a solid phase at higher density. In this paper we examine ^{4}He and the charged-Bose gas for both infinitesimal and noninfinitesimal deviations from the liquid wave function. We find that considerable information on the location and nature of the liquid-solid phase transition may be obtained with very little effort from calculations on the liquid alone. Constrained HNC calculations of a solid phase using nonspherically symmetric correlation function confirm the association between the behavior of the energy surface near the liquid phase and the structure of the solid phase. The method is recommended for other systems; ^{4}He and the Coulomb gas are quite different, but it gives transitions in these systems.

I. INTRODUCTION

At zero temperature, some boson systems crystallize while others remain liquid. Considerable effort has been spent in trying to determine, from first principles, the nature of the ground state for a given system. The Monte Carlo solution of the many-body Schrödinger equation is probably the most elegant approach and leads to numbers which may be compared with experiment.[1,2] Chief among other methods, the Rayleigh-Ritz principle has been applied with a number of interesting variations. One virtue of this method is that, to varying degrees, certain aspects of the calculation may be performed analytically.

For the liquid phase, many variational calculations have been based on a Jastrow[3] ansatz for the wave function. For the solid, one wishes to incorporate at least some aspects of lattice structure in the wave function, and this has usually been done by writing the variational wave function as the product of two-body correlation factors times a lattice wave function. Koehler[4–7] suggested a form for the lattice factor of the wave function which is a generalization of a product of Gaussians confining particles to lattice sites. In the absence of explicit pair correlations, this wave function allows calculations to be made in a straightforward fashion; the inclusion of pair correlations in Jastrow form greatly complicates the calculation of expectation values. These computations have been performed in the past by Monte Carlo means, e.g., Ref. 8, truncation of the cluster expansion at the two-body level, Refs. 6, 9, and 10, or by the use of integral equations to sum certain classes of cluster diagrams.[11]

The above approaches have all incorporated explicitly the crystal aspects of the wave function with the use of single-particle wave functions or the correlated lattice structure advocated by Koehler. Feenberg[12] proposed that the explicit use of single-body wave functions was unnecessary for describing solids. He suggested that one could build up good solid wave functions from products of pair, triplet, and higher correlation functions. These would generate a solid without either definite orientation or position. Roughly speaking, the pair correlations keep particles apart and the triplets produce a latticelike ordering without referring to external axes. This basis puts liquid and solid wave functions on a more equal footing.

Our own interests in the problem of crystallization arise from detailed study of the liquid using a simple Jastrow wave function and the hypernetted-chain (HNC) approximation to the radial distribution function. The corresponding approximate energy functional has some useful features. In addition to yielding relatively reliable approximations to the energies of quantum fluids, it also serves as a stable basis for optimization. Variation of the approximate energy functional leads to an Euler-Lagrange equation for the distribution function[13–15] which may be solved by one

means[16] or another.[17] These solutions yield good estimates of the pressure and compressibility as a function of density.[18] Furthermore, for only a little investment of effort beyond that made in computing the optimal distribution function, one may gain rather substantial returns.

In Ref. 19, we showed that for ^{4}He, the stationary solutions for the distribution function corresponded to energy minima and linked the linear behavior of the liquid structure function at small k to the positivity of the compressibility. From a determination of the eigenvalue spectrum and eigenfunctions for small deviations from the optimal distribution function, we observed interesting features of ^{4}He at low densities (near the spinodal point) and high (above the experimental solidification density) densities. At low density, one particular eigenvalue drops rapidly toward zero at the spinodal point; its eigenfunction was seen to correspond to puddling in the system. At high density, a single nonspherically symmetric eigenfunction was observed to lie substantially below all other eigenfunctions, and we speculated that this might be a sign of incipient crystallization. On the basis of this observation, we were led to infer various features of the solid from the behavior of the energy functional at the liquid minimum.

The purpose of the present paper is to establish that there is a basis for making these inferences and to show to what degree these inferences are reliable. We choose a variational wave function which allows a smooth mapping of the energy surface from the liquid minimum to a very crystalline structure. The wave function used to describe the solid is in fact the same as that for the liquid; however the correlation function is no longer assumed to be spherically symmetric. No single-particle lattice wave function is introduced. In spirit, this wave function is close to that of Feenberg,[12] but the relative spatial orderings are now achieved with direction-dependent pair correlation functions rather than with three-body correlations. There are several advantages to this choice. First, the variational wave function remains properly symmetric as it ranges from liquid to solid phases. Second, we can directly exploit our rather complete knowledge of the behavior of the energy functional in the liquid limit to direct the search with nonspherical correlation functions. Latticelike ordering may be introduced without the complications which would arise with three-body functions. Finally, the use of the same form for both liquid and solid wave functions enables us to say as much as possible about the solid after doing only the liquid calculation.

In Sec. II, we review the behavior of the energy functional near the liquid minimum. The example discussed in this section is ^{4}He, although similar remarks could be made for other systems since studied. Section III investigates the most simple-minded path in the energy surface and finds that for ^{4}He, it only goes upward. The method for producing a crystallinelike wave function which reduces to a low-eigenvalue result for small deviations from the liquid is presented in Sec. IV. The results of such a calculation are presented for ^{4}He in Sec. V and for the charged-Bose gas in Sec. VI. In Sec. VI, we also mention the eigenvalue properties of the homework potential. There remains for Sec. VII an assessment of the usefulness of the eigenvalue and eigenvector analysis and the limitations of the HNC energy functional for solid energy calculations.

II. OPTIMAL HNC FOR A LIQUID

Consider an infinite system of bosons of mass m interacting via a two-body potential $V(r)$. With a variational wave function of the Jastrow form

$$\psi = \prod_{i<j} f(\vec{r}_{ij}) \tag{1}$$

the energy per particle may be expressed in the Jackson-Feenberg[19] form as

$$E = \frac{\rho}{2}\int d\tau g^{1/2}\left[\frac{-\hbar^2}{m}\nabla^2 + V(r) - \frac{\hbar^2}{4m}\nabla^2 \ln\left[\frac{f^2}{g}\right]\right] g^{1/2} \tag{2}$$

for a real but not necessarily spherically symmetric f. In the HNC approximation, the radial distribution function $g(\vec{r})$ is related to the correlation function f by

$$\ln\left[\frac{f^2}{g}\right] = -F\left[\frac{(S-1)^2}{\rho S}\right] , \tag{3}$$

where $F(y)$ denotes the Fourier transform of the function y and the liquid structure function $S(\vec{k})$ is given by

$$S(\vec{k}) = 1 + \rho F(g-1) . \tag{4}$$

With this approximation, the energy functional may be recast as

$$E[g(\vec{r})] = \frac{\rho}{2}\int d\tau g^{1/2}\left[\frac{-\hbar^2}{m}\nabla^2 + V + F\left[\frac{-\hbar^2 k^2}{4m\rho}\frac{(S-1)^2}{S}\right]\right] g^{1/2} . \tag{5}$$

This functional, which does not assume spherical symmetry for f, is the basis for the remainder of the work to be described in this paper.

Previously, we found local minima of the energy functional of Eq. (5) for liquid ^{4}He at various densi-

ties.[19] The corresponding $g(r)$ and $S(k)$ are shown in Fig. 1 at densities of $\rho = 0.018, 0.030$ Å^{-3}. Indications of instability are seen by examining the change ΔE induced by small changes in $g^{1/2}(r)$. For small perturbations, this study leads to a linear eigenvalue equation, in which the positivity of all eigenvalues is a guarantee of stability. The motion of eigenvalues and the form of eigenfunctions at the densities given foreshadow changes in phase at more extreme densities where actual calculations are precluded by numerical indelicacies.[19] At a density of 0.030 Å^{-3}, the structure of $g(r)-1$ already extends out to about 50 Å, where $g(r)-1 \approx 10^{-7}$. At somewhat higher densities, the ringing structure in $r^4(g-1)$ observed in Ref. 19 is expected to extend much further out. While there seems to be no trouble, in principle, in extending the HNC calculation to higher density, the benefit to be gained from such solutions is incommensurate with the effort which would be required to obtain them. At lower density, a particular eigenvalue plummets toward zero. The corresponding eigenfunction has $k \approx 0$ and is associated with the steep slope of $S(k)$ for small k and the vanishing of the compressibility at the spinodal point. At higher density, a different eigenvalue moves discretely below the continuum toward zero. Its eigenfunction has a finite k related to the maximum in the liquid structure function. Other manifestations of its presence are long-range oscillations in $g(r)$ and an increase in the peak value of $S(k)$. In the next section, we show that these features, although very suggestive, will not lead to a lowering of the energy without the inclusion of some crystalline structure.

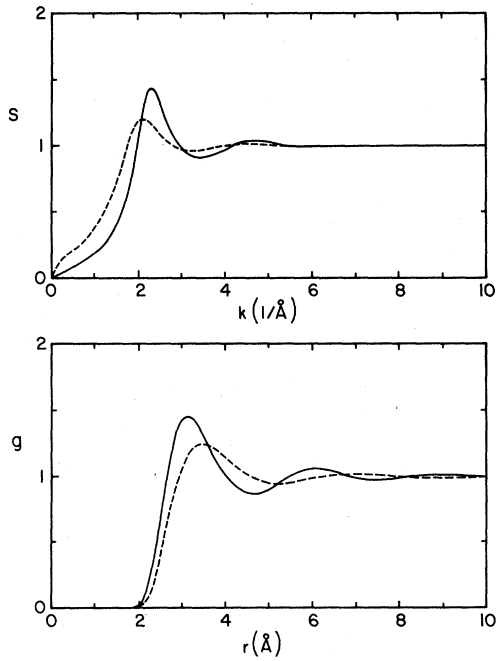

FIG. 1. The liquid structure function $S(k)$ and distribution function $g(r)$ are shown for densities $\rho = 0.018$ Å^{-3} (broken curves) and $\rho = 0.030$ Å^{-3} (solid curves).

III. SMALL DEVIATIONS FROM THE OPTIMAL HNC SOLUTION

Around a liquid minimum, the energy may be expanded as[18]

$$E[g] = E[g_0] + \tfrac{1}{2}\rho \int \delta g^{1/2} K \delta g^{1/2} d\tau \ , \tag{6}$$

where

$$\delta g^{1/2} = \tfrac{1}{2}(g - g_0) g^{-1/2} \ ,$$

$$Ky = \left[\frac{-\hbar^2}{m}\nabla^2 + V + F\left[\frac{-\hbar^2 k^2 (2S_0+1)(S_0-1)^2}{4m\rho S_0^2}\right]\right] y$$

$$- g_0^{1/2}\left[F\left[\frac{\hbar^2 k^2 (S-1)^3}{4mS^3}\right]\right] * (g_0^{1/2} y) \ , \tag{7}$$

and the "$*$" in Eq. (7) denotes a convolution integral, and the term linear in δg vanishes for an extremal function g_0. For all physical systems studied, the eigenvalues of the kernel K have been positive and the corresponding energies are thus local minima. All infinitesimal variations δg give higher energies, but some choices are more favorable than others. We may quantify this by examining the soft modes at the minimum, i.e., by studying the eigenvalues and eigenvectors of the kernel K. A set of radial eigenvectors y_{lk} may be found from the uncoupled equations

$$K y_{lk}(r)\, Y_{lm}(\theta, \phi) = \lambda_{lk} y_{lk}(r)\, Y_{lm}(\theta, \phi) \ . \tag{8}$$

The Y_{lm} are the usual spherical harmonics, and $y_{lk}(r)$ and λ_{lk} are independent of m. For infinitesimal variations, the smallest change in energy for a given normalization N,

$$N^2 = \int d\tau (\delta g^{1/2})^2 \tag{9}$$

occurs when $\delta g^{1/2}$ is proportional to the lowest eigenfunction of K, and

$$\Delta E = \tfrac{1}{2}\rho \lambda_{\min} N^2 \ . \tag{10}$$

Simple estimates of the eigenvalue spectrum may be made when the l is sufficiently large that the potential term V is essentially screened by the angular momentum barrier in Eq. (7). With this assumption, the y_{lk} form a continuum with

$$y_{lk} \sim j_l(kr)\, Y_{lm}(\theta, \phi); \quad \lambda_{lk} \cong \frac{\hbar^2 k^2}{mS^3(k)} \ . \tag{11}$$

Given the linear behavior of $S(k)$ for small k and

the fact that $S(k)$ approaches unity for large k, the approximate continuum spectrum will have a minimum at some k_m, will be doubly degenerate above that, and will be independent of l at a given k.

Clearly, the condition for a given $\delta g^{1/2}$ to be "soft" is that it be a linear combination of the y_{lk} with k approximately equal to k_m. For ^{4}He at $\rho = 0.030$ Å^{-3}, the approximate eigenvalue minimum occurs at $k_m = 2.25$ Å^{-1} with $\lambda_0 = 21.2$ K. Although Eq. (11) is strictly valid only in the large-l limit, the calculated continuum for $0 \leq l \leq 12$ actually begins at $\lambda = (22.1 \pm 0.3)$ K. Equation (11) evidently provides a good estimate of λ_l for all l. The *ad hoc* extension of Eq. (11) to small l is less reliable; since for small l, $j_l(kr)$ does not look like the actual eigenfunction at small r; the actual eigenfunction looks rather like $g_0^{1/2}$ in order to screen the potential.

In addition to the continuum eigenvalue spectrum, there is a discrete eigenvalue in the $l = 5$, 6, and 7 channels. The $l = 6$ eigenvalue falls farthest below the continuum as the density increases; at $\rho = 0.030$ Å^{-3}, it is down to 80% of the continuum limit. The corresponding eigenfunction y_{6*} looks at large distances like an exponentially damped sinusoid with period determined by k_m and damping related to the distance below the continuum of the discrete eigenvalue and the curvature of the continuum spectrum as a function of k at the minimum. This behavior is familiar from bound-state wave functions, where the corresponding quantities are the binding energy and $\hbar^2/m$.

Extrapolation of this eigenvalue with density suggested that it might vanish at $\rho = 0.050$ Å^{-3}, where the energy would still be a minimum for spherically symmetric changes in $g(r)$ but not for nonspherically symmetric changes.[19] Calculations of $g(r)$ at densities above 0.030 Å^{-3} are very difficult and have not been performed.

The combination of high density and nonspherically symmetric correlation functions suggests a liquid-solid phase transition. Since low-temperature ^{4}He is known to crystallize into a close-packed (hcp) structure, it is natural to see whether the eigenfunction y_{6*} reflects this. However, the hcp structure does not possess inversion symmetry, so an adequate δg would require admixtures of the $l = 5$ and $l = 7$ eigenfunctions as well. Since these could come in with varying relative coefficients, any conclusions which might be drawn would be weakened by the availability of these two parameters. Instead, we consider only lattice structures with a cubic point-group symmetry; fcc, bcc, and sc. For these structures, the odd-l functions are not appropriate. We expect fcc results to differ only insignificantly from hcp results, since both structures describe close-packed systems. In addition, at finite temperature there is a transition in solid ^{4}He to an fcc phase. There is a unique linear combination of $Y_{6m}(\theta, \phi)$ invariant under these symmetry operations: the "Kubic harmonic"[20]

$$C_6(\theta, \phi) = \left[-\frac{1}{\sqrt{8}} Y_{60}(\theta, \phi) + \sqrt{\frac{7}{16}} [Y_{64}(\theta, \phi) + Y_{6-4}(\theta, \phi)] \right] . \quad (12)$$

The product of this angular function with the radial function y_{6*} at $\rho = 0.030$ Å^{-3} has no free parameters. The contours of this function are displayed on a cube with one face cut away in Fig. 2. The side of the cube is chosen so that a regular fcc lattice with that lattice constant has a ^{4}He density of 0.030 Å^{-3}. The close coincidence of the peaks in $\delta g^{1/2}$ with many of the fcc lattice sites is striking.

Of course, for small admixtures of this eigenfunction, the energy still increases. Our first hope was that for larger variations, the cubic and higher terms might bend the energy surface downward. To try this, we used Eq. (5) to evaluate the energy for arbitrarily large variations proportional to $y_{6*}(r) C_6(\theta, \phi)$. As shown in Fig. 3, this hope was short-lived. This path on the energy surface, although paved with good intentions, led upward even more rapidly than the parabolic curve suggested by Eq. (10). This behavior persisted when spherically symmetric variations were simultaneously allowed. The reason for this failure is that for large perturbations, it is not sufficient to have the limited angular dependence of Eq. (12). It is necessary that the admixture be coherent over more than just a few of the nearest-neighbor sites. For example, the third- and fifth-nearest-neighbor directions lie nearly at nodes of the angular function of Eq. (12), and hence cannot contribute effectively to the energy. We also note that the chaining opera-

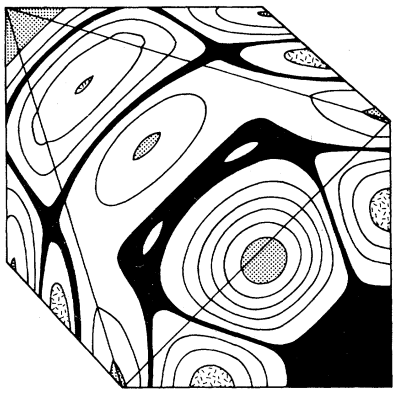

FIG. 2. Contours of $y_{6*}(r) C_6(\theta, \phi)$ are shown on a cube whose side corresponds to the lattice spacing for an fcc lattice at density $\rho = 0.030$ Å^{-3}. The solid areas represent areas near nodes in either y_{6*} or C_6; the dotted areas are peaks, while the dashed areas are troughs. The origin is in the lower right-hand corner.

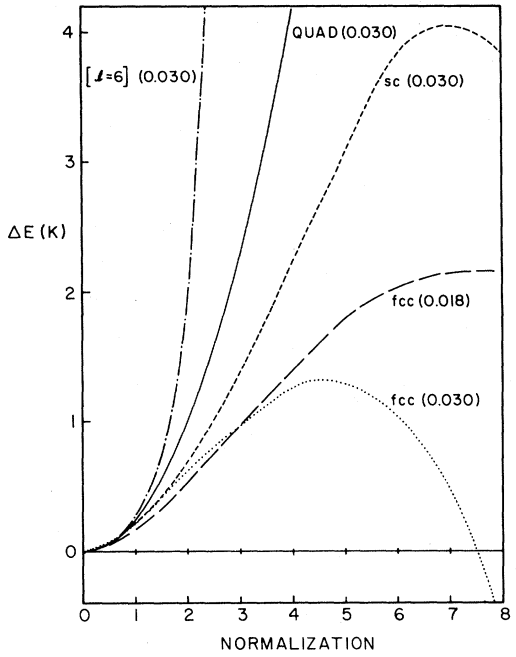

FIG. 3. The increase in energy over the liquid phase, ΔE, is shown for various trial wave functions as a function of the normalization. The curve labeled "$[l=6]$" is for the eigenfunction $y_{6*}(r)C_6(\theta,\phi)$, while the curve labeled "QUAD" is for the same function in the quadratic approximation. The remaining curves are labeled by the crystal structure and the density.

tions constructing g from f are likely to produce enhanced periodic behavior in g. The availability of other l eigenfunctions at the same k and with only slightly higher λ_l suggests the use of standing plane waves, as in a crystal.

We wish to emphasize that the study of small perturbations only serves as a guide for subsequent calculations. For positive eigenvalues, the energy expression given by Eq. 10 is a parabola opening upward. In the calculations discussed in the remaining sections, the assumption of small perturbations is set aside and the full nonlinear (in δg) Eq. (5) is used to calculate the energy.

IV. LARGE DEVIATIONS FROM THE OPTIMAL HNC SOLUTION

At this point, we know the location of a path leading gently away from the liquid minimum in the energy surface. In this section, we derive a form for δg which has one end firmly embedded in a crystalline region yet is flexible enough to represent the early steps of the path quite well. The wave function could have been built up as a sum of low-lying radial eigenfunctions multiplied by their corresponding crystal harmonics. As mentioned in Sec. III, the behavior of the y_{lk} is approximately that of a screened $j_l(kr)$ and λ_{lk} is roughly independent of l. This suggested a simpler alternative in which a crystalline form is first constructed from plane waves with $k \simeq k_m$; short-range correlations are then imposed on top of this to simulate the behavior of y_{lk} at small r. The resulting paths on the energy surface will be useful provided that for one of them the energy eventually turns over and starts decreasing as the f becomes less and less spherically symmetric.

In principle, we can change both the spherical and nonspherical parts of $g(\vec{r})$, but in the present calculation, only the nonspherical part is allowed to change. We start with a lattice structure for $\delta g(\vec{r})$, and then remove objectionable properties until the final δg is suitable. At that point, we may subtract the angle-averaged (and hence spherically symmetric) part.

Consider a lattice with vectors $\vec{R}_{abc}$ and a function $\delta g(\vec{r})$ given by

$$\delta g(\vec{r}) = \sum_{abc} p(\vec{r} - \vec{R}_{abc}) \tag{13}$$

$$= C \sum_{abc} D_{abc} \exp(i\vec{K}_{abc} \cdot \vec{r}) \ , \tag{14}$$

where C is a normalization constant, $\vec{K}_{abc} = k_0(a\hat{x} + b\hat{y} + c\hat{z})$ is a vector in the reciprocal space (the integers a,b,c depend on the lattice type), and D_{abc} is the Fourier transform of $p(\vec{r})$ evaluated at K_{abc}. Aside from the short-range behavior, the plane waves in the sum in Eq. (14) are nearly eigenfunctions of the kernel of Sec. II with eigenvalues $\lambda_k = \hbar^2 K_{abc}^2/mS^3(K_{abc})$. If the dominant term in Eq. (14) comes from a K_{abc} which is near the minimum of the continuum, k_m, and the D_{abc} fall off rapidly with K, then $\delta g(\vec{r})$ is approximately a linear combination of the lowest continuum eigenfunctions with phases guaranteed to be consistent locally with the lattice structure. The form of Eq. (14) must be polished, however. The screening needed for the hard core must be simulated, the spherically symmetric part removed, and the oscillations damped for large r to prevent S from becoming singular. [A pure plane wave would lead to delta functions in $S(\vec{k})$]. Keeping in mind these restrictions, we obtain

$$\delta g(\vec{r}) = Ag_0(r)\exp(-\mu r) \times \sum_{abc} D_{abc}[\exp(i\vec{K}_{abc} \cdot \vec{r}) - j_0(K_{abc}r)] \ , \tag{15}$$

where the D_{abc} and K_{abc} are independent of the signs and permutations of the abc. The first four K_{abc} are tabulated in Table I for fcc, bcc, and sc lattices. For the particular case that $p(r)$ is a Gaussian, then D_{abc} is given by

$$D_{abc} = \exp(-K_{abc}^2\sigma^2/2) \ . \tag{16}$$

TABLE I. The first few K_{abc} are shown for three crystal lattices in units of k_0.

abc	lattice fcc	bcc	sc
001			1
011		$\sqrt{2}$	$\sqrt{2}$
111	$\sqrt{3}$		$\sqrt{3}$
002	2	2	2
012			$\sqrt{5}$
112		$\sqrt{6}$	
022	$\sqrt{8}$	$\sqrt{8}$	
113	$\sqrt{11}$		

The parameters D_{abc} and k_0 may be freely varied. The parameter μ must be constrained to prevent singularities in $S(\vec{k})$, and the parameter A must be restricted so that $g(\vec{r})$ and $S(\vec{k})$ do not pass through zero in any direction. If either of these latter conditions were violated, it would be obvious that g could not come from *any* wave function.

The leading term of Eq. (15) will roughly agree with the lowest eigenvector if

$$K_{abc}^{\min} = k_m \tag{17}$$

which gives $k_0 = (k_m/\sqrt{3}, k_m/\sqrt{2}, k_m)$ for the (fcc, bcc, sc) lattices. The densities corresponding to these k_0's are $\rho_0 = (k_0/2\pi)^3$ (4,2,1) or $\rho_0 = (k_m/2\pi)^3 \times (0.77, 0.71, 1.0)$. One might guess that the best crystal structure will be one for which the ρ_0 calculated from k_m corresponds closely to the density of the system. Numerical results, which follow, show that this is true, so that a knowledge of $S(k)$ substantially correct for the liquid would indicate strongly the crystal structure of the solid!

In plotting the energy, it is useful to summarize the various parameters by a single number. Thus, we plot the change in energy away from the liquid as a function of the normalization. In the case considered, the energy with $\delta g(r)$ given by Eq. (15) is given quite well for small normalization by a parabola which lies only slightly above that of the lowest discrete eigenvalue. This justifies the procrustean techniques used in obtaining Eq. (15) from Eq. (14).

Further justification of the form of Eq. (15) requires specific calculations of the energy and a check that the parameters which minimize the energy at a given normalization are plausible. For example, if p is taken to be a Gaussian which falls to half its peak value at a quarter of the nearest-neighbor spacing, then for an fcc lattice, $D_{002}/D_{111} = 0.64$, $D_{022}/D_{111} = 0.11$, and $D_{113}/D_{111} = 0.028$. Similar values may be obtained for other assumptions about the behavior of p.

V. HELIUM

At zero temperature, ^{4}He liquid saturates at a density of 0.022 Å^{-3}; at $\rho = 0.029$ Å^{-3}, it crystallizes into a close-packed hcp structure. There is a small region of bcc solid at about 1.5 K, and at substantially higher pressures and temperatures an fcc phase is stable. A sc phase has not been found.

Equation (15), with spherically symmetric g, predicts saturation at $\rho \cong 0.017$ Å^{-3} with the Lennard-Jones potential.[18] Calculations with nonspherically symmetric g's have been performed at densities of 0.018 and 0.030 Å^{-3}, the latter lying above the experimental solidification density. The sc, bcc, and fcc structures have been tried. For each density with a given lattice, the energy shift and normalization were computed for different choices of D_{abc}, k_0, and A. The parameter μ was fixed at 0.2 Å^{-1}. At fixed normalization, we observed a minimum in the energy shift with respect to variations of D_{abc} and k_0; the value of A was then determined by the normalization. At small N, only the D_{abc} corresponding to the smallest K_{abc} was nonzero; in the quadratic region, only the lowest eigenvalue is desired. At larger normalization, other reciprocal-lattice vectors become significant.

The minimum energy shift is shown in Fig. 3 as a function of the normalization. The curves labeled "QUAD" and "$[l=6]$" have been discussed in Sec. III and set the scale for the present curves. At $\rho = 0.030$ Å^{-3}, there is evidence of solidification in the fcc energy. The curve rises to a low maximum of about 1.3 K, well under the 5.3 K for the parabola at the point, and then falls off and actually goes below zero. The plotted energy stops near the point in which $g(\vec{r})$ or $S(\vec{k})$ develops a zero in some direction.

In contrast, at lower density, $\rho = 0.018$ Å^{-3}, the energy shift does not turn over. Also, the $\rho = 0.030$ curve with sc structure only shows a hint of turning over before g or S becomes unphysical, and the energy shift is much higher than for the fcc lattice. The bcc lattice calculations, not illustrated, lie between the sc and fcc cases. We note that this ordering of the curves is the same as one would infer from the packing fraction in these three cases.

We now consider in more detail the parameters at a density of $\rho = 0.030$ Å^{-3}. At this density, the computed k_m was 2.25 Å^{-1}. For (fcc, bcc, sc) lattices at this density, Eq. (17) would suggest $k_m = (2.13, 2.19, 1.95)$ Å^{-1}. The first two lattices require little "stretching" to conform to the minimum eigenvalue, while the sc lattice is quite far off. Figure 4 shows the sensitivity of the fcc energy shift to the k_0 at different normalizations. The contours in this figure are drawn with increasing intervals, so that if the quadratic approximation were good and the energy were independent of k_0, all contours would be

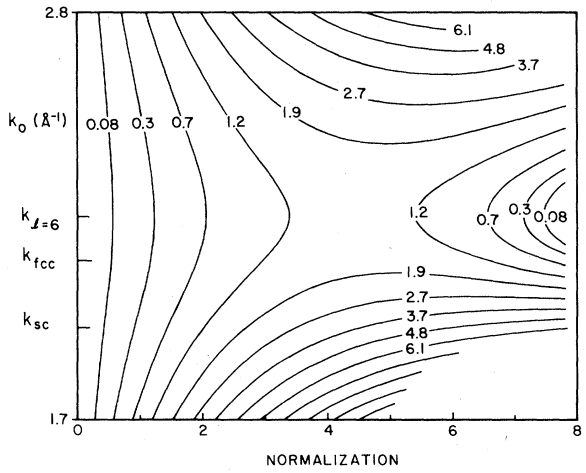

FIG. 4. For a density of $\rho = 0.030$ Å^{-3} and the fcc structure, this contour plot shows the dependence of the energy on the k_0 parameter and the normalization. The contours are labeled by the increase in energy over the liquid minimum. Note that the contours are not equally spaced.

vertical and equally spaced. This is useful in compressing the scale, but might lead one to underestimate the steepness of the ridges leading down to the saddle. It is apparent that the path leading to the top of the saddle which one would like to follow is the one corresponding to k_m and not to k_{fcc} or k_{sc}. However, since k_{fcc} and k_m differ by about 5%, this is quite acceptable. Even in the region where the quadratic approximation breaks down completely, the k_0 one should use is determined by the lowest eigenfunction at the liquid minimum.

Another indication that our distribution function is trying to describe a crystal comes from the parameters D_{002}, D_{022}, and D_{113}. For an fcc structure, the higher density, and at the peak in the energy curve of Fig. 3, the optimum ratios of D_{002}/D_{111}, D_{022}/D_{111}, and D_{113}/D_{111} are 0.65, 0.10, and 0.028, in rough agreement with Eq. (16) and a lattice site smearing which falls to half the peak value at a quarter of the nearest-neighbor spacing.

Finally, in Figs. 5 and 6 we show contour plots of $g(\vec{r})$. The first shows the spherically symmetric g_0 on the faces of a cube which has been cut across one face. A helium atom is given at the lower right-hand corner, and the contours are at constant values of $g(\vec{r})$. In rather striking contrast, Fig. 6 shows the distribution function at the peak in the energy curve of Fig. 3. The distribution function has maxima at or near the fcc lattice sites. It should be emphasized that the size of the cube is determined solely by the density while the contour plots are for the trial $g(\vec{r})$ from Eq. (15) with parameters obtained by minimizing the energy at the value of the normalization.

If g or S becomes negative at any point, it can no longer come from a wave function. The energies, in the region of such a point, should not be imbued with particular significance, as they are probably too dependent on details of the nonspherical distribution function. The saddle point, where the energy turns down again, appears to be rather insensitive to minor changes in the g and hence is a more stable indication of an impending phase transition.

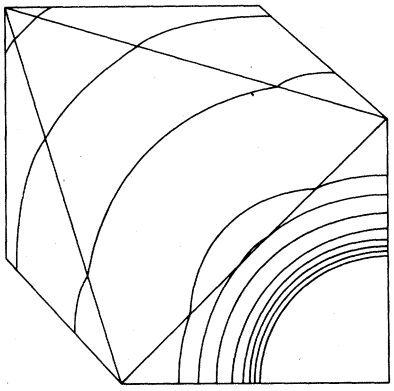

FIG. 5. The contours of $g(\vec{r})$ for the liquid minimum at $\rho = 0.030$ Å^{-3} are shown on the surface of a cube with the (111) face exposed. A helium atom is present in the lower right-hand corner.

All calculations presented were performed at a value of $\mu = 0.2$ Å^{-1}. This parameter may not be allowed to vary freely, as it would try to exploit shortcomings in the approximate energy functional. The value of μ must not be too large if one wishes to include a reasonable amount of long-range order, but it must be small enough to keep g and S positive.

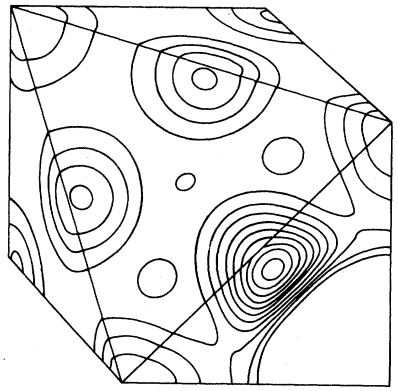

FIG. 6. The contours of $g(\vec{r})$ for the fcc wave function at the saddle point of Fig. 3 at a density of $\rho = 0.030$ Å^{-3} are shown on the surface of a cube with (111) face exposed. The wave function is obtained by minimizing the energy functional, while the size of the cube is determined by the density.

We do not expect the true energy to depend sensitively on distant neighbors, so a constrained μ is not unreasonable. The value of μ used gives an e-folding distance corresponding to the second-nearest-neighbor positions in an fcc lattice. The height of the curve is somewhat sensitive to the value of μ chosen, although μ can be decreased to the 0.15 Å^{-1} suggested by the decay rate of the discrete $l=6$ eigenfunction without changing the results qualitatively. Further assessments of the sensitivity of the results to μ could be performed by evaluating some of the elementary diagram corrections to Eq. (5) or using Monte Carlo techniques to evaluate the energy. Either method could be used to select a proper value of μ.

VI. CHARGED BOSONS

The boson Coulomb gas in a neutralizing background is of interest because it crystallizes at low, rather than high densities. At low densities, the lattice energy goes like $-q^2\rho^{1/3}$ (attractive), while the localization energy goes like $\rho^{2/3}$. For small enough density, the first term dominates and the system crystallizes. The coefficients of the lattice energy in the classical limit are obtained with the method of Coldwell-Horsfall and Maradudin.[21] For (bcc, fcc, hcp, sc) lattices, they are (1.444 23, 1.444 14, 1.444 08, and 1.418 65). At low densities, therefore, the matter should crystallize into a bcc phase.

For this potential, the energy functional of Eq. (5) must be modified slightly to remove the otherwise infinite contribution which is cancelled by the uniform background. This is performed simply with the replacement of the term $\int g v d\tau$ by $\int (g-1) v d\tau$. For a system of particles with charge e, there are two independent length scales. An average interparticle spacing is given by $r_0=(\frac{4}{3}\pi\rho)^{-1/3}$, and the Bohr radius is $a_0=\hbar^2/me^2$. There is no additional range associated with the potential, so that for any $\hbar^2/m$ and ρ, the energy may be obtained by scaling an energy calculated with the same ratio of $r_s=r_0/a_0$. Large values of r_s correspond to low densities. It is convenient to calculate the energy in units where $\hbar^2/m=r_0=1$, and thus $\rho=3/(4\pi)$. With this convention, the Coulomb interaction is

$$V(r)=\frac{r_s}{r} \quad . \tag{18}$$

The matter is solid for $r_s > r_{sc}$; numerous calculations of r_{sc} suggest that it is difficult to determine but on the order of a hundred. The present situation is summarized in Ref. 2; the precise value of r_{sc} does not concern us here.

Solutions of the Euler-Lagrange equation in the Coulomb problem have rather different character from those obtained for short-range potentials. In particular, $S(k)$ must vanish as k^2 for small k. As a result, k^2/S^3 must behave as k^{-4} for small k, and hence its transform behaves linearly at large r. This leads to erratic numerical behavior. To circumvent this problem, we made the decision to cut a little off the tail of the potential, i.e.,

$$V(r)=\frac{r_s}{r}\exp(-\beta r) \quad . \tag{19}$$

The value β was reduced until we could no longer obtain high-quality numerical solutions in reasonable time; the final value adopted was $\beta=0.3$. Since the induced screening of the bare potential has stronger effects, this is primarily a technical point. Alternatively, one could solve the Euler-Lagrange equation by imposing boundary conditions at a small value of r and neglecting edge effects. As β is reduced, the $g(r)$ soon changes by only very small amounts; the primary difference is seen in the (very) small-k behavior of $S(k)$.

In the uniform limit,[13] where $g \simeq 1$, the Euler-Lagrange equation may be solved for $S(k)$:

$$S(k)=\frac{k^2}{(k^4+12r_s)^{1/2}} \quad . \tag{20}$$

Our estimate for the lowest eigenvalue is then obtained by minimizing k^2/S^3 to obtain

$$\lambda_m=9\sqrt{r_s} \quad . \tag{21}$$

The uniform limit should be good for small r_s (large density). At $r_s=2$, the uniform limit predicts $\lambda_m=12.7$, while our calculation gives $\lambda_m=10.3$. The λ_m increases until $r_s \simeq 20$, and then begin to fall again, in spite of Eq. (21). Extrapolation of $\lambda_m/(9\sqrt{r_s})$ suggests that a continuum eigenfunction may drop through zero at $r_s \simeq 300$.

Below the continuum there are discrete eigenvalues. For $r_s=2(5)$, the $l=0, 2(2)$ eigenvalues are slightly below the other λ_l, but there is no sign of damping in the corresponding eigenfunction in a box of size 20. For $r_s=20$, there appears a discrete eigenvalue at $l=4$; at $r_s=100$, the lowest discrete eigenvalue is at $l=6$ and lies about 7% below the continuum. The $l=4$ and $l=8$ eigenvalues are also somewhat below the continuum at that r_s. The appearance of the nonspherically symmetric eigenfunctions suggests a nearby crystalline phase.

As in the case of helium, the lowest eigenfunction alone leads to a path on the energy surface which does not turn over. The use of Eqs. (5) and (15) gives paths which lie appreciably lower than that obtained with the lowest eigenfunction alone. The energy shifts are shown in Fig. 7 for bcc, fcc, and sc lattices at $r_s=20$ and $r_s=100$. The value of $\mu=0.4$ used was obtained by scaling that used for the ^{4}He calculation. The behavior of these curves is similar to that obtained for ^{4}He. The lowest curves corre-

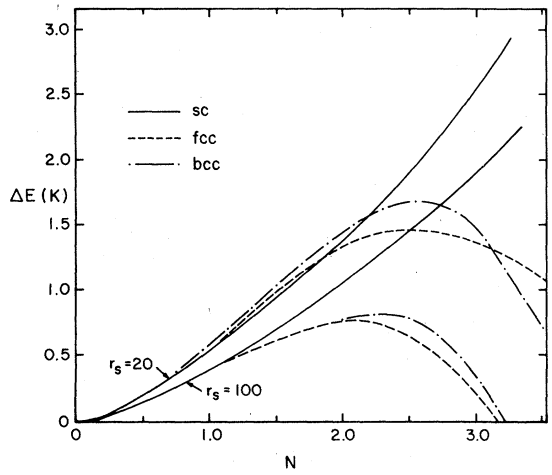

FIG. 7. The increase in energy over the liquid phase, ΔE, is shown for the Coulomb gas at $r_s = 20$ and $r_s = 100$ for three lattice structures as a function of the normalization, N.

spond to the fcc and bcc lattices whose energies are virtually indistinguishable, and the larger value of r_s. The sc curves do not turn over at all. In contrast to ^{4}He, the sensitivity of the height of the maximum of the curve to the lattice constant is reduced. This is presumably an indication that the cause of crystallization in the Coulomb gas is more subtle than the hard core of the ^{4}He potential. The constraint parameter μ could be varied without changing the qualitative picture, but the details such as the value of r_s at which crystallization might occur, depend on it too sensitively to justify further computation.

VII. DISCUSSION

The Jastrow ansatz in the HNC approximation has been used extensively in the study of quantum liquids. We have demonstrated that the extension of this wave function to real, nonspherically symmetric correlation functions can also provide a qualitatively correct description of the solid at the same density. For two extremely different systems, liquid ^{4}He and the Coulomb gas, this wave function generates the right behavior of the energy with respect to increases in density and the choice of crystal structure. The approximations made in obtaining Eq. (5) remove the variational aspect of the problem and hence mandate a constrained (fixed) calculation.

The present calculations were motivated by the optimal Jastrow-HNC calculations of simple liquids where we were tempted to regard vanishing eigenvalues in the second-order variational calculation as indicators of physically interesting phase transitions rather than artifacts of the approximations. The calculations presented here, as well as previous discussions of collapsing liquids at low densities, suggest that there is no reason to resist this temptation. Given the reliability of the approximate expression, Eq. (11), for the lowest continuum eigenvalues, it is possible to make qualitatively useful statements regarding the existence of phase transitions and crude estimates of densities before which they will have taken place given only the optimal liquid structure function at a number of densities. This level of calculation requires no additional computation. In well-studied systems such as liquid ^{4}He and the Coulomb gas, this information may be of little value. However, in systems such as nuclear matter and neutron star matter, where the underlying interaction is imperfectly known, qualitative information of the kind obtained in this manner may be useful. In addition to standard liquid-solid phase transitions, nuclear and neutron matter may have abnormal phases which exploit the strong tensor component of the nucleon-nucleon interaction or pion-condensed phases. Indeed, indications of premature phase transitions can help in excluding inadequate models of the nucleon-nucleon interaction.

Such simple estimates of the lowest continuum eigenvalue, although appealingly simple, have nothing to say about the possible existences of discrete eigenvalues or the nature of the new phase. For this, one must actually solve the eigenvalue equation, Eq. (8). This level of calculation requires only the kernel already used in optimizing the distribution function. In both liquid ^{4}He and the Coulomb gas, the softest variations of the correlation functions about the liquid minima are found to be nonspherically symmetric and strongly suggest particular crystal structure. The present results show that, while calculations valid only in an infinitesimal neighborhood of the (locally) stable liquid can never *produce* a solid, the nature of the eigenvalue spectrum and the form of the lowest eigenfunctions *are* a good basis for predictions of the nature of the solid. By constructing the variational wave function, we have shown explicitly how the information obtained at the liquid point can be used in describing the solid. In both systems studied, the full wave function did somewhat better than a simple analysis of k^2/S^3. In helium, matching the k_m with crystal structure and density would have suggested a bcc structure. The behavior of the $l = 6$ eigenfunction, however, indicated a preference for fcc structure. In the Coulomb problem, the k_m preferred an fcc structure, while the calculations indicated no real preference for fcc over bcc. In both cases, the calculations indicated no real preference for fcc over bcc. In both cases, the calculations are in substantial agreement with experiment.

The present method is not competitive with Monte Carlo calculations in determining transition densities, because the approximations made require some constraint. Once a specific constraint is imposed, it may

be supported either by showing that it gets the right answer or by estimating its effect. As Miller *et al.*[11] have shown, even the existence of a solid is sensitive to the choice of constraint (with a somewhat different wave function); thus there is little point in using the present method in trying to make quantitative predictions. Rather, it should be used as a tool in understanding the change of the wave function over the phase transition. There remains, of course, the interesting question of how the present correlation function, obtained from the nonspherically symmetric g by Eq. (3) would do in an exact variational (Monte Carlo) calculation. Such a calculation would be welcome.

The problem of metastable states and nucleation has been considered in applications to superfluidity[22] and superconductivity[23]; further discussion may be obtained from Ref. 24. The approach of these papers may be useful in combination with the present work in investigating the process of crystallization and freezing times.

In other systems, particularly where the interaction is not completely known, qualitative information of the type obtained with this method may be useful. Nuclear matter and neutron star matter are examples of such liquids. The richness of the interaction allows the possibility of pion condensation as well as solidification. The present calculation suggests that it may be useful to study some properties of these systems by carefully examining the normal liquid phase.

Finally, the somewhat unexpected ability of Jastrow-HNC calculations to generate phase transitions provides an additional measure of confidence in calculations of the normal liquid. Features of the distribution function which ultimately lead to solidification or low-density collapse can play an important, although not necessarily dominant, role in the liquid even near its equilibrium density. The present results suggest that such features are at least approximately incorporated in optimal HNC-Jastrow calculations.

ACKNOWLEDGMENTS

The work presented here was sponsored, in part, by the USDOE under Contract No. EY-76-S-02-3001. A. L. would like to thank SUNY at Stony Brook for its hospitality while portions of this work were being carried out; R. A. S. is grateful to the Rijksuniversiteit Groningen for a most pleasant visit during the early part of this work.

[1]P. A. Whitlock, D. M. Ceperley, G. V. Chester, M. H. Kalos, Phys. Rev. B 19, 5598 (1979).
[2]D. M. Ceperley and M. H. Kalos, in *Monte Carlo Methods in Statistical Physics,* edited by K. Binder (Springer, Berlin, 1979).
[3]R. Jastrow, Phys. Rev. 98, 1479 (1955).
[4]T. R. Koehler, Phys. Rev. 144, 789 (1966).
[5]T. R. Koehler, Phys. Rev. Lett. 17, 89 (1966).
[6]T. R. Koehler, Phys. Rev. Lett. 18, 654 (1967).
[7]T. R. Koehler, Phys. Rev. 165, 942 (1968).
[8]J. P. Hansen and E. L. Pollock, Phys. Rev. A 5, 2651 (1972).
[9]C. -W. Woo and W. E. Massey, Phys. Rev. 177, 272 (1969).
[10]D. N. Lowy and C. -W. Woo, Phys. Rev. D 13, 3201 (1976).
[11]M. D. Miller, W. J. Mullin, and R. A. Guyer, Phys. Rev. B 18, 3189 (1978).
[12]E. Feenberg, J. Low Temp. Phys. 16, 125 (1974).
[13]E. Feenberg, *Theory of Quantum Fluids* (Academic, New York, 1969).
[14]L. J. Lantto and P. J. Siemens, Phys. Lett. 68B, 308 (1977).
[15]A. Kallio and R. A. Smith, Phys. Rev. Lett. 68B, 315 (1977).
[16]C. Chang and C. E. Campbell, Phys. Rev. B 15, 4238 (1977).
[17]L. J. Lantto, A. D. Jackson, and P. J. Siemens, Phys. Lett. 68B, 311 (1977).
[18]A. D. Jackson, A. Lande, and L. J. Lantto, Nucl. Phys. A 317, 70 (1979).
[19]L. Castillejo, A. D. Jackson, B. K. Jennings, and R. A. Smith, Phys. Rev. B 20, 3631 (1979).
[20]F. C. von der Lage and H. A. Bethe, Phys. Rev. 71, 612 (1947).
[21]R. A. Coldwell-Horsfall and A. A. Maradudin, J. Math. Phys. 1, 395 (1960).
[22]J. S. Langer and M. E. Fisher, Phys. Rev. Lett. 19, 560 (1967).
[23]J. S. Langer and V. Ambegaokar, Phys. Rev. 164, 498 (1967).
[24]J. S. Langer, Phys. Rev. Lett. 21, 973 (1968).